Journal of http://www.satursonpublishing.com/
Research in Multidisciplinary Methods and Applications
ISSN 2957-3920 (Online) ISSN 3007-7060 (Print)
Volume 4, Issue 1, January 2025

Design and Aerothermal Simulation of Radar Ventilation Ducts in Aircraft Environmental Control and Cooling Systems

Hang Yang, Luqiang Zhao, Xuefei An

College of Engineering, Zunyi Normal University, Zunyi, Guizhou, 563006, China

*Corresponding to: Hang Yang

Abstract: Radar ventilation ducts in aircraft environmental control and cooling systems operate under complex aerodynamic and thermal conditions. The duct geometry usually includes a diffuser section, a straight transition section, and a curved outlet, which may cause non-uniform pressure distribution and local flow separation. In this paper, a three-dimensional model of a radar ventilation duct is established, and the internal flow field is simulated by computational fluid dynamics. The static pressure distribution, velocity field, and convergence behavior of the numerical solution are analyzed. The simulation results show that the static pressure decreases gradually from the inlet to the curved outlet, and a low-pressure region appears near the bend. The pressure difference between the inlet and outlet is significant under the present boundary conditions, which indicates that the duct configuration has a considerable influence on the aerothermal performance. The residual curves show that the solution converges after a certain number of iterations, and the continuity and momentum residuals remain at a low level. A table of key aerodynamic parameters is provided, and several governing equations are used to describe the flow and heat transfer behavior. The results can provide reference for the design and optimization of radar ventilation ducts in aircraft environmental control systems.

Keywords: radar ventilation duct; environmental control system; aerothermal simulation; computational fluid dynamics; static pressure; flow field

1 INTRODUCTION

Aircraft environmental control systems are responsible for cabin pressurization, temperature control, and avionics cooling. Among the various subsystems, radar ventilation ducts play an important role in removing heat from radar equipment and maintaining the operating temperature within a safe range [1]. Unlike ordinary ventilation ducts, radar ventilation ducts are usually installed in a confined space and are subject to strict requirements on pressure loss, flow uniformity, and thermal performance. Therefore, the design of such ducts requires a detailed understanding of the internal flow field and pressure distribution.

In recent years, many studies have focused on the flow and deposition behavior in ventilation ducts. Sippola [1] investigated particle deposition in ventilation ducts and provided experimental data for duct flow analysis. Cross [2] studied active control of sound in ventilation ducts, which is related to the acoustic performance of duct systems. Sippola and Nazaroff [3] developed a model for particle loss in ventilation ducts and discussed the influence of duct geometry on particle transport. Paurobally et al. [4] further examined active noise control in ventilation ducts. Adam et al. [5] studied aerosol deposition in ventilation ducts and analyzed the deposition characteristics under different flow conditions. These studies mainly focus on particle deposition, noise control, and aerosol transport, while the aerothermal performance of radar ventilation ducts with curved outlets has received less attention.

The present work aims to fill this gap by establishing a three-dimensional computational fluid dynamics model of a radar ventilation duct. The duct consists of a diffuser inlet, a straight section, and a curved outlet. The static pressure distribution and flow field characteristics are simulated. The convergence behavior of the numerical solution is also examined. The results are expected to provide useful information for the design of aircraft environmental control and cooling systems.

Journal of http://www.satursonpublishing.com/
Research in Multidisciplinary Methods and Applications
ISSN 2957-3920 (Online) ISSN 3007-7060 (Print)
Volume 4, Issue 1, January 2025

2 Physical Model and Numerical Method

2.1 Geometric Model

The radar ventilation duct considered in this study is shown in Fig. 1. The duct can be divided into four parts: the inlet diffuser, the middle transition section, the straight pipe, and the curved outlet. The inlet has a larger diameter, and the cross-section gradually contracts along the flow direction. The outlet is bent upward to match the installation space in the aircraft.

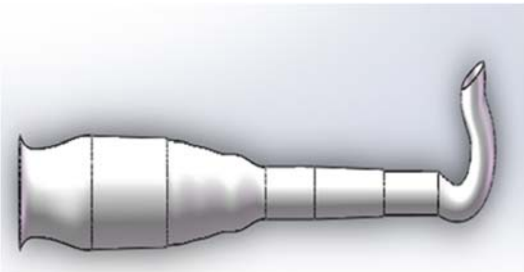

Fig. 1. Three-Dimensional Geometric Model Of The Radar Ventilation Duct.

The main geometric parameters are listed in Table 1. The total length of the duct is about one point two meters, and the maximum diameter of the inlet is about zero point two five meters. The outlet diameter is about zero point zero eight meters. The bend angle of the outlet is about ninety degrees.

Table 1. Main Geometric Parameters Of The Radar Ventilation Duct

Parameter	Symbol	Value	Unit
Total length	L	1.2	m
Inlet diameter	D1	0.25	m
Outlet diameter	D2	0.08	m
Length of diffuser	L1	0.35	m
Length of straight section	L2	0.55	m
Bend angle	theta	90	degree
Wall thickness	t	0.002	m

2.2 Governing Equations

The flow in the duct is assumed to be steady, incompressible, and turbulent. The governing equations include the continuity equation, the momentum equation, the energy equation, and the turbulence model equations.

The continuity equation is written as:

$$\frac{\partial \rho}{\partial t} + \nabla \cdot (\rho \mathbf{u}) = 0 \quad (1)$$

For steady incompressible flow, Eq. (1) can be simplified as:

$$\nabla \cdot \mathbf{u} = 0 \quad (2)$$

The momentum equation is:

$$\rho(\mathbf{u} \cdot \nabla)\mathbf{u} = -\nabla p + \mu \nabla^2 \mathbf{u} + \mathbf{F} \quad (3)$$

where rho is the density, u is the velocity vector, p is the static pressure, mu is the dynamic viscosity, and F is the body force.

The energy equation is:

$$\rho c_p(\mathbf{u} \cdot \nabla T) = \nabla \cdot (k \nabla T) + \Phi \quad (4)$$

where c sub p is the specific heat at constant pressure, T is the temperature, k is the thermal conductivity, and Phi is the viscous dissipation term.

The standard k-epsilon turbulence model is used to close the equations. The turbulent kinetic energy k and its dissipation rate epsilon are given by:

$$\rho(\mathbf{u} \cdot \nabla k) = \nabla \cdot \left[\left(\mu + \frac{\mu_t}{\sigma_k}\right) \nabla k\right] + G_k - \rho \varepsilon \quad (5)$$

where mu sub t is the turbulent viscosity, sigma sub k is the turbulent Prandtl number for k, and G sub k is the generation of turbulent kinetic energy due to the mean velocity gradient.

2.3 Boundary Conditions and Numerical Settings

The inlet boundary condition is set as a velocity inlet. The inlet velocity is twenty meters per second, and the inlet temperature is three hundred kelvin. The outlet boundary condition is set as a pressure outlet, and the outlet static pressure is zero gauge pressure. The wall is assumed to be adiabatic and no-slip. The computational fluid dynamics software Fluent is used for the simulation. The SIMPLE algorithm is adopted for pressure-velocity coupling. The second-order upwind scheme is used for the convection terms. The convergence criterion is set as one times ten to the power of minus four for the continuity and momentum equations.

3 Results and Discussion

3.1 Static Pressure Distribution

Journal of http://www.satursonpublishing.com/
Research in Multidisciplinary Methods and Applications
ISSN 2957-3920 (Online) ISSN 3007-7060 (Print)
Volume 4, Issue 1, January 2025

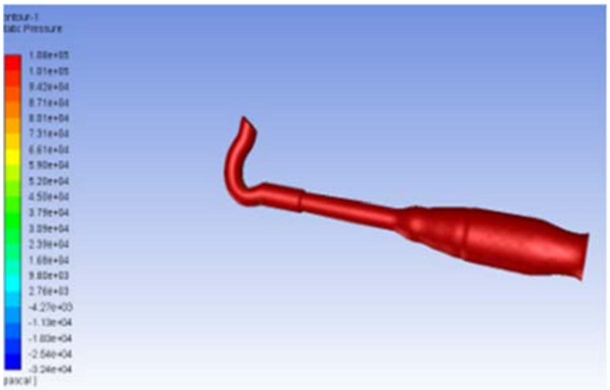

FIG. 2. STATIC PRESSURE DISTRIBUTION IN THE RADAR VENTILATION DUCT.

Figure 2 shows the static pressure distribution in the radar ventilation duct. It can be seen that the static pressure is highest at the inlet and decreases gradually along the flow direction. The maximum static pressure is about one point zero eight times ten to the power of five pascals, and the minimum static pressure is about minus three point two six times ten to the power of four pascals. The pressure difference between the inlet and outlet is about one point nine times ten to the power of five pascals.

The pressure drop is mainly caused by the following factors. First, the cross-section of the duct contracts from the inlet to the outlet, which leads to an increase in flow velocity and a decrease in static pressure according to Bernoulli's principle. Second, the curved outlet causes a local flow separation and a secondary flow, which increases the local pressure loss. Third, the friction between the fluid and the duct wall also contributes to the pressure drop.

From Fig. 2, it can also be observed that the pressure distribution is not uniform in the bend region. A low-pressure region appears near the inner side of the bend, while a relatively high-pressure region appears near the outer side. This is consistent with the characteristics of curved pipe flow. The non-uniform pressure distribution may affect the cooling performance of the radar equipment and should be considered in the design of the duct.

3.2 *FLOW FIELD CHARACTERISTICS*

The velocity field is closely related to the pressure distribution. In the inlet diffuser, the flow velocity is relatively low because of the large cross-sectional area. As the flow enters the transition section, the velocity increases gradually. In the straight section, the velocity profile becomes more uniform. In the curved outlet, the velocity increases further, and a secondary flow is generated due to the centrifugal force.

The Reynolds number at the inlet is:

$$Re = \frac{\rho u D}{\mu} \tag{6}$$

Using the inlet diameter and inlet velocity, the Reynolds number is about three point four times ten to the power of five, which indicates that the flow is fully turbulent. Therefore, the standard k-epsilon model is suitable for this simulation.

The mass flow rate can be calculated by:

$$\dot{m} = \rho A u \tag{7}$$

where A is the cross-sectional area. The mass flow rate at the inlet is about zero point nine eight kilograms per second. The outlet mass flow rate is approximately equal to the inlet mass flow rate, which satisfies the mass conservation.

3.3 *CONVERGENCE BEHAVIOR*

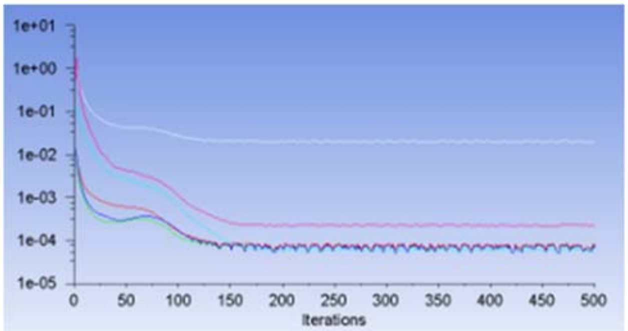

FIG. 3. RESIDUAL CURVES OF THE NUMERICAL SIMULATION.

Figure 3 shows the residual curves of the numerical simulation. The residuals decrease rapidly in the first fifty iterations and then gradually level off. After about one hundred and fifty to two hundred iterations, the residuals of continuity and momentum equations remain below one times ten to the power of minus four. The energy residual also reaches a stable level. This indicates that the numerical solution is convergent and the results are reliable.

The convergence behavior also shows that the flow field in the duct is relatively stable. No obvious oscillation is observed in the residual curves, which suggests that the steady-state assumption is reasonable for the present study. However, if the flow rate changes rapidly or the outlet is subject to a time-varying back pressure, a transient simulation may be needed in future work.

3.4 *AEROTHERMAL PERFORMANCE*

The aerothermal performance of the duct can be evaluated by the pressure loss coefficient and the heat transfer coefficient. The pressure loss coefficient is defined as:

$$K = \frac{\Delta p}{\frac{1}{2}\rho u^2} \tag{8}$$

where delta p is the pressure difference between the inlet and outlet. Using the present results, the pressure loss coefficient is about two point five. This value is relatively high, which indicates that the duct configuration should be optimized to reduce the pressure loss.

The heat transfer coefficient can be estimated by:

$$h = \frac{q}{T_w - T_f} \tag{9}$$

where q is the heat flux, T sub w is the wall temperature, and T sub f is the fluid temperature. In the present simulation, the wall is assumed to be adiabatic, so the heat transfer coefficient is not directly calculated. In future work, a conjugate heat transfer model will be used to evaluate the cooling performance of the duct.

TABLE 2. KEY AERODYNAMIC PARAMETERS OF THE RADAR VENTILATION DUCT

Parameter	Symbol	Value	Unit
Inlet velocity	u1	20	m/s
Outlet velocity	u2	62.5	m/s
Inlet static pressure	p1	1.08e5	Pa
Outlet static pressure	p2	-3.26e4	Pa
Pressure difference	delta p	1.9e5	Pa
Reynolds number	Re	3.4e5	—
Mass flow rate	m dot	0.98	kg/s
Pressure loss coefficient	K	2.5	—

4 CONCLUSIONS

In this paper, a three-dimensional computational fluid dynamics simulation of a radar ventilation duct in an aircraft environmental control and cooling system is carried out. The main conclusions are as follows.

The static pressure decreases gradually from the inlet to the outlet. The pressure difference between the inlet and outlet is significant. A low-pressure region appears near the inner side of the curved outlet.

The flow velocity increases from the inlet to the outlet due to the contraction of the cross-section. The Reynolds number at the inlet indicates that the flow is fully turbulent.

The residual curves show that the numerical solution converges after a certain number of iterations. The continuity and momentum residuals remain at a low level, which indicates that the results are reliable.

The pressure loss coefficient is relatively high. The duct configuration should be optimized to reduce the pressure loss and improve the aerothermal performance.

In future work, the conjugate heat transfer and the effect of different turbulence models will be considered. The particle deposition and noise characteristics will also be studied to provide a more comprehensive evaluation of the radar ventilation duct.

FUNDING

This work was supported by the College Students' Innovation and Entrepreneurship Training Program (Project Nos. S202510664976, S202510664982, S202510664987, and S2025106641000).

REFERENCES

[1] Sippola M R. Particle deposition in ventilation ducts[J]. Office of Scientific & Technical Information Technical Reports, 2002. DOI:10.2172/810494.

[2] Cross C F. Active control of sound in ventilation ducts[J]. Industrial Noise, 2024. DOI:10.25144/22043.

[3] Sippola M R, Nazaroff W W. Modeling particle loss in ventilation ducts[J]. Atmospheric Environment, 2003, 37(39): 5597–5609. DOI:10.1016/j.atmosenv.2003.07.016.

[4] Paurobally M R, Sassi S, Renno J. Active control of noise in ventilation ducts[C]//International Congress on Sound and Vibration, 2019.

[5] Adam N, Everitt P, Riffat S B. Aerosol deposition in ventilation ducts[J]. International Journal of Energy Research, 1996, 20(12): 1095–1101.